Geoenvironmental Disasters

RESEARCH

Open Access

Plugging efficiency of pouring aggregates through multiple boreholes into an inundated tunnel to prevent groundwater inrush disasters

Shuang Hui[1,2], Wanghua Sui[1*], Gailing Zhang[1], Jiaxing Chen[1,3] and Shibo Yu[4]

Abstract

This paper presents an experimental investigation of the plugging efficiency of aggregate pouring through multiple boreholes under flowing water conditions into an inundated mine tunnel. Aggregate pouring into an inundated mine tunnel has been widely used and constitutes the premise for the salvage of flooded underground mines through further grouting. However, corresponding in-depth research is relatively limited due to the concealment of underground engineering. A visual experimental setup for aggregate pouring into a tunnel replica was built based on the theory of similarity between sediment movement and slurry pipeline transportation. Four factors, each with four levels, including the aggregate particle size (0.25–0.5, 0.5–1, 1–2 and 2–5 mm), distance between boreholes (0.5, 0.75, 1 and 1.5 m), initial water flow rate (0, 1.5×10^{-2} m/s, 2.4×10^{-2} m/s and 3×10^{-2} m/s) and tunnel inclination (0°, 3°, 5° and 8°) were selected in orthogonal experiments to investigate the plugging efficiency. Range and variance analysis of the four-level orthogonal array experimental results indicated that the factors influencing the plugging efficiency, varying between 83.96 and 98.15%, could be ranked in descending order as the initial water flow rate, aggregate particle size, distance between boreholes and tunnel inclination. The former two factors yielded a more significant influence than that of the latter two factors. The measured water pressure difference ranging from 16 to 32% between the front and back ends of the formed aggregate mass in the pouring process indicated that there remained a high resistance to water flow, even if the aggregate mass was not capped but reached a certain length. Plugging criteria for aggregate pouring into horizontal and inclined tunnels were then proposed. Moreover, the optimal distance between boreholes to form an effective bulkhead was determined, which could be defined as the distance between boreholes when the aggregate mass exhibits the fastest build-up and the plugging capacity is reached.

Keywords: Inundated tunnel, Groundwater inrush disaster, Plugging efficiency, Aggregate pouring, Critical velocity, Sedimentation, Plugging criterion

Introduction

Grouting and sealing projects for emergency relief in inundated mine tunnels are usually implemented in two stages: aggregate pouring and grouting. Figure 1 shows a schematic of the aggregate pouring and grouting processes in an underground coal mine tunnel for inundation mitigation. The purpose of the aggregate pouring stage is to form an accumulated aggregate section in the tunnel to transform pipeline flow into permeate flow. The purpose of the grouting stage is to reinforce the aggregate section with cement grout to eliminate water flow (Jiang et al. 2020). Therefore, to achieve efficient sealing, the first stage plays an important role in successful salvage efforts. Table 1 lists successful cases of this method in emergency relief and salvage of mines by pouring aggregates and subsequent grouting. In the treatment

*Correspondence: suiwanghua@cumt.edu.cn

[1] School of Resources and Geosciences, Institute of Mine Water Hazard Prevention and Control Technology, China University of Mining and Technology, Xuzhou 221116, China
Full list of author information is available at the end of the article

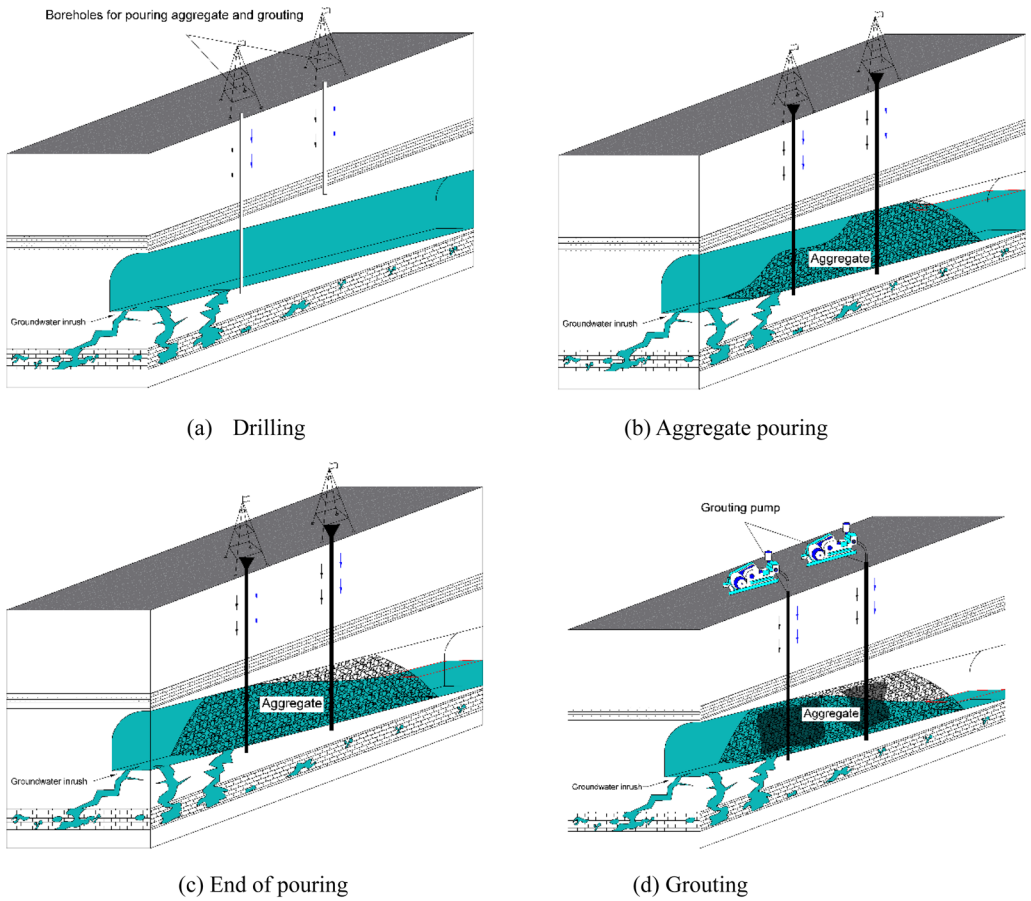

Fig. 1 Schematic of the aggregate pouring and grouting processes for water inrush disaster treatment in a coal mine

of extra-large water inrush disasters, a resistance section with a length of several hundred meters is generally needed.

To choose appropriate parameters for groundwater inrush disaster control using this approach, pouring trials should be conducted before aggregate pouring if the unit water injection exceeds $10–20 \times 10^{-3}$ m^3/min·m. In pouring trials, different particle sizes, water–solid mass ratios and pouring rates should be systematically considered and explored. The literature indicates that the process of aggregate accumulation and plugging in tunnels can be divided into three stages: the bottom laying stage, filling stage and plugging stage (Wang 2012; Mou et al. 2020). This division of plugging stages was based on analysis; this division has not been verified in practice or via laboratory testing. It has been found that the aggregate pouring speed and particle size should be continuously adjusted to further reduce the seepage speed and create favorable conditions for grouting after successful capping. At this time, the water head difference between the two sides should be increased so that the slurry can propagate along the aggregate accumulation mass and improve the blocking effect (Zhang et al. 2020). Integrated technology, differences and difficulties of bulkhead construction involving aggregate pouring and grouting in a tunnel under flowing water conditions were examined via a comparison to the general pregrouting method. The evaluation of the hydrogeological conditions of the inundated mine and identification of water sources, geological structure, cause of water inrush disasters and technical flood control methods were considered (Guo 2005; Jiang 2009; Li 2010).

Innovative methods and materials have been used in recent years in the construction of plugging sections in inundated tunnels, such as grouting involving directional drilling boreholes (Shao et al. 2011; Ji 2014; Wang et al. 2011). A successful project of water-conducting pathway plugging in a karst collapsed column completely eliminated groundwater flow along the main horizontal direction with 4 horizontal branch boreholes for aggregate pouring into the subsurface and subsequent cement grout injection (Zheng 2018). Other examples include

Table 1 Case histories of groundwater inrush disaster treatment in mine tunnels via aggregate pouring in China

Coal mine	Time of accident occurrence	Groundwater resources and pathway	Pressure (MPa)	Flowrate (m^3/h)	Time of aggregate pouring	Aggregate consumption (m^3)	Cement grouts ($\times 10^3$ kg)	Sealing effect (%)
Longmen coal mine, Henan	11 December 1994	Cambrian karst aquifer, through a geologic structure	3.0	2,200.0	20 June–22 August 1994	3100.5	757.0	97.1
Renlou coal mine, Anhui	4 March 1996	Ordovician karst collapsed column	5.0	11,854.0–34,570.0	25 April–25 May 1996	129.9	15,032.0	85.0–90.0
Wucun coal mine, Henan	15 November 1999	Ordovician karst aquifer intersected by faults and collapsed column	N/A	2,145.0, 2,378.0 (maximum)	18 January to 10 March 2000	1,535.0	3,182.6	97.0–100.0
Dongpang coal mine, Hebei	12 April 2003	Ordovician karst collapsed column	5.0	7,000.0	10 May–11 June 2003	42,837.0	26,396.0	98.7
Sanshuping coal mine, Shaanxi	7 August 2011	Ordovician karst aquifer	3.0	8,000.0, 13,200.0 (maximum)	15 October–9 November 2011	25,716.0	60,383.0	98.7
Taoyuan coal mine, Anhui	2 February 2013	Karst collapsed column	N/A	30,000.0	24 February–16 May 2013	N/A	220,843.0	100.0
Panji coal mine No. 2, Anhui	25 May 2017	Ordovician karst collapsed column	N/A	3,024.0	20 June–27 July 2017	21,141.0	15,349.0	100.0
Yiliang Mining Company, Yunnan	2 March 2019	Permian Maokou and Qixia Formation aquifers	N/A	1,650.0	15 June–30 October 2019	3900.0	910.0	98.0

successful plugging with an efficiency of 99% in the Luotuoshan coal mine, Inner Mongolia, and Yuchang coal mine, Shaanxi, and the successful use of the method of grouting bag emplacement to achieve rapid and controllable blocking of tunnels under high flow rates (Wang et al. 2013; Zhu 2015).

Experimental investigation and numerical simulation methods are commonly used methods to better understand the mechanism of aggregate accumulation and grouting sealing in inundated underground tunnels. Experiments of aggregate pouring into a horizontal pipeline through a single borehole indicated that the influencing factors of the plugging efficiency in descending order are the aggregate particle size, initial water flow velocity, and water–solid mass ratio (Wang et al. 2013; Li 2010; Zhang et al. 2020). A large-scale model was designed with opaque materials considering a water pressure of 5 MPa to simulate the movement of grout-conserving bags under high-pressure conditions (Dong et al. 2020). Numerical simulations with the computational fluid dynamics (CFD) technique have been widely conducted in the investigation, design and management of slurry pipe flow in recent years, such as the Eulerian–Lagrangian method, two-fluid model (TFM) and CFD–DEM (discrete element method) coupled method (Ekambara et al. 2009; Kaushal et al. 2012; Capecelatro and Desjardins 2013; Messa et al. 2014; Arolla and Desjardins 2015; Messa and Malavasi 2015; Uzi and Levy 2018; Messa and Matoušek 2020; Mou 2021).

To provide a theoretical reference and better understand the movement and deposition of aggregates in tunnels, existing studies of slurry flow in pipelines are helpful because of the similarity between aggregate accumulation in tunnels and slurry hydraulic transport in pipelines (Wilson 1979). Durand (1952) classified the state of solid–liquid mixtures into three categories, i.e., homogeneous, intermediate, and heterogeneous mixtures, based on suspension flow of sand and gravel in water. Wasp et al. (1977) categorized the flow regime of solids in pipelines into homogeneous and heterogeneous types. Fei (1994) divided solid particles into bed loads and suspended loads. Soepyan et al. (2013) and Zouaoui et al. (2016) investigated the transport of sand-water slurries along a horizontal pipeline, and Miedema (2016) determined the transition of slurry flow from heterogeneous

into homogeneous flow. There exists an important concept to define the state of deposition and movement of particles in fluid. The critical velocity has been defined as the minimum velocity of water at which aggregate particles transition from a static state to a moving state regarding aggregate pouring in tunnels (Zhang et al. 2020). Similar terms have been proposed for slurry transportation in pipelines. The concept of the limit deposit velocity was used by Durand (1952) to denote the critical deposit velocity, and a representative Durand equation was provided. The critical flow rate was proposed and defined as the velocity at which solid particles are deposited from a suspended state to produce a fixed bed (Graf et al. 1970). Fei (1994) defined the critical velocity of water as the velocity at which aggregate particles can be transported without settling. In accordance with the assumptions of Thomas (1979), a model for the prediction of the deposition velocity of a slurry comprising fine particles was developed by Wasp and Slatter (2004). A semiempirical equation to predict the critical deposit velocity was proposed (Pinto et al. 2014), and the effects of the pipeline shape, particle size and inclination angle on the critical flow velocity were investigated (Kim et al. 2008; Bratland 2010; Corredor et al. 2016). Moreover, the reduction in pressure along the pipeline can be used to evaluate friction loss in two-phase flow (Newitt et al. 1955; Turian et al. 1971; Turian and Yuan 1977; Ni et al. 1989; Vlasak et al. 2012; Miedema 2015). The hydraulic gradient is influenced by many factors, such as the particle size, specific gravity and fluid viscosity (Duckworth and Argyros 1972; Allahvirdizadeh et al. 2016). However, water pressure changes and distribution along tunnels in the multiple-borehole pouring process and the influence on the formation of water-blocking segments have not yet been thoroughly investigated.

In summary, the abovementioned theoretical, experimental and numerical studies were fundamental to explain the accumulation and plugging mechanism for groundwater control and salvaging. However, in-depth research is relatively limited and lacks universality due to the concealment of underground engineering. For example, the actual process of aggregate sedimentation during pouring should be further investigated despite the proposed division into three stages. The interaction between aggregate pouring into different boreholes and the borehole layout should be further examined. Because multiple boreholes are usually used to achieve better and swifter plugging in practical projects, there exist few cases describing the use of a single borehole. Factors such as the distance between boreholes and tunnel inclination should be considered in orthogonal array design (OAD) experiments to study aggregate sedimentation, migration and accumulation and criteria for plugging effects. Consequently, the main purpose of this study was to experimentally investigate the plugging effects of aggregate pouring through multiple boreholes under flowing water conditions in an inundated mine tunnel using a visual test platform. Different factors influencing the plugging effect of aggregates and the sedimentation and accumulation mechanism of aggregates were analyzed based on the experimental results. The results indicated that the initial water flow velocity and aggregate particle size exert a more significant influence on the plugging efficiency than that of the distance between boreholes and tunnel inclination. The water pressure difference between the front and back ends of the formed aggregate mass indicates resistance against water flow. In addition, this paper proposed a plugging criterion for aggregate pouring and the optimal distance between boreholes to establish an effective bulkhead. The results can facilitate a better understanding of the effects of aggregate accumulation mass formation, water pressure loss and aggregate pouring into multiple boreholes on the plugging efficiency.

Materials and methods

Similarity

Pipeline flow of solids represents a special case of pipeline dynamics. This model is a nonconstant flow pipeline transportation model completely filled with fluid and solids. It is difficult to achieve complete pipeline geometric similarity to the test requirements. The Froude criterion (gravity similarity criterion), Reynolds criterion and Euler criterion are commonly used similarity criteria in fluid modeling. Previous investigation and analysis studies of pipeline hydraulic simulation models have indicated that tunnels containing moving water can be mainly considered with the Euler and gravity similarity criteria, followed by the Reynolds criterion. Therefore, the gravity similarity criterion was used for hydraulic simulation of a flooded tunnel. The fluid in this test was clean water with a temperature of approximately 7 °C. The Reynolds number $Re > 2000$ was calculated according to the minimum water flow velocity of approximately 1.5×10^{-2} m/s. Therefore, the flow state was turbulent in this test. The tunnel wall generally comprises concrete material with a roughness ratio ranging from 0.014 to 0.017, and plexiglass with a roughness ratio of 0.008–0.0095 was used in this test. According to the gravity similarity criterion, the roughness ratio could be obtained as $\lambda_n = \lambda_L^{\frac{1}{6}}$. This indicates that the geometric ratio should be higher than 1:30 to meet the gravity similarity criterion (Chanson 2008). Therefore, a geometric ratio between the model and prototype of 1:20 was selected after comprehensive consideration of the laboratory facilities and similarity (Yalin 1971). Based on previous research results and similarity

criteria, a pipeline was simulated with a cross-sectional area of 12 m^2, a length of 80 m and a water inrush flow of 6440 m^3/h. Table 2 lists the scale of different parameters.

Factors and materials

The test parameters were determined referring to the cases listed in Table 1.

Aggregate particle size *A*. The aggregate particle size in the experiments was selected at the four levels of 0.25–0.5 mm, 0.5–1 mm, 1–2 mm and 2–5 mm. These levels were determined according to the similarity rule and on-site investigation of general coal mine water blocking projects, where the selected aggregates included yellow sand (0.7–3.0 mm), rice-sized and centimeter-scale stone (3–5 mm), melon seed-sized stone (5–10 mm) and slag particles (10–20 mm). Sand and gravel particles were screened and washed to remove finer soil particles and impurities to ensure a high visualization clarity of the aggregate movement process.

Distance between boreholes *B*. According to the layout of grouting and blocking boreholes in submerged tunnels, multiple boreholes are required for pouring and grouting, and the distance between boreholes generally varies between 15 and 30 m. The distance was selected at four levels, namely, 0.5 m, 0.75 m, 1 m and 1.5 m, according to the geometric scale in this study. Figure 2c shows details of the borehole layout in this test.

Initial water flow rate *C*. In flooded tunnels, plugging sections are generally selected in concentrated waterways, exhibiting high water flow rates. For example, in the Dongpang coal mine in Hebei, the flow rate in the water inrush tunnel reached as high as 13.88×10^{-2} m/s, and the flow rate in Panji coal mine No. 2 in Anhui reached 7×10^{-2} m/s. In this test, the flow rate scaling ratio is 4.47, and the initial water flow rate in the orthogonal array was set at four levels: 0, 1.5×10^{-2} m/s, 2.4×10^{-2} m/s and 3×10^{-2} m/s.

Tunnel inclination *D*. In rescue operations in flooded mines, grouting and blocking are mostly selected in horizontal or uphill tunnels relative to the movement direction of water flow. In this experiment, the tunnel inclination was selected at the 4 levels of 0°, 3°, 5° and 8°.

The aggregate injection rate in this test is the rate generated by the gravitational action of water flow and aggregates. The rate is proportional to the length of the pouring borehole. If sidewall friction is ignored, the final rate at which aggregates enter the tunnel is $v = \sqrt{2gh} = 3.13$ m/s, where h is the distance from the top surface of the water–sand mixture in the funnel to the top of the tunnel.

Table 2 Model scale set based on the Froude criterion

Scale for	F_r
Inertial force/gravity	v^2/Lg
Length λ_L	$\lambda_L = 20$
Time λ_t	$\lambda_L^{\frac{1}{2}} = 4.47$
Flow velocity λ_v	$\lambda_L^{\frac{1}{2}} = 4.47$
Flow quantity λ_Q	$\lambda_L^{\frac{5}{2}} = 1788.85$
Pressure λ_p	$\lambda_L = 20$
Force λ_F	$\lambda_\rho \lambda_L^3 = 8000$
Power λ_P	$\lambda_\rho \lambda_L^{\frac{7}{2}} = 35777$
Roughness λ_n	$\lambda_L^{\frac{1}{6}} = 1.65$

Experimental setup

The plugging efficiency of aggregate injection into a submerged tunnel under water flow is affected by many factors, including natural and engineering factors, such as the tunnel inclination, water flow rate, distance between boreholes, aggregate particle size, water–solid mass ratio and injection rate. The experimental setup could provide a constant water head and adjustable and recyclable water flow conditions at different flow rates. The system could control the water–solid mass ratio and aggregate pouring rate. A data collection system could collect flowrate and water pressure data in real time. Images of aggregate accumulation and migration in the pipeline were captured for process analysis. Figure 2 shows a schematic and photo of the experimental setup.

Orthogonal array for experiment design

Table 3 provides an orthogonal array with four factors, each with four levels. Hence, $L_{16}4^5 = 16$ trials are needed in this experiment. The array was designed according to the OAD method proposed by C. R. Rao and used in industrial experimentation by Taguchi (Hedayat et al. 1999).

Results and analysis

Plugging efficiency

Residual water flow channel

Under static water conditions, the resulting aggregate accumulation mass is tapered due to the angle of repose. The cross section of the simulated tunnel model is circular, and the contact conditions between the aggregates and pipe wall cannot be completely matched, resulting in a gap between the accumulation mass and pipe inner wall, namely, a residual water flow channel (Zhang et al. 2020).

The residual water flow channel can be divided into a minimum residual channel and a final residual channel.

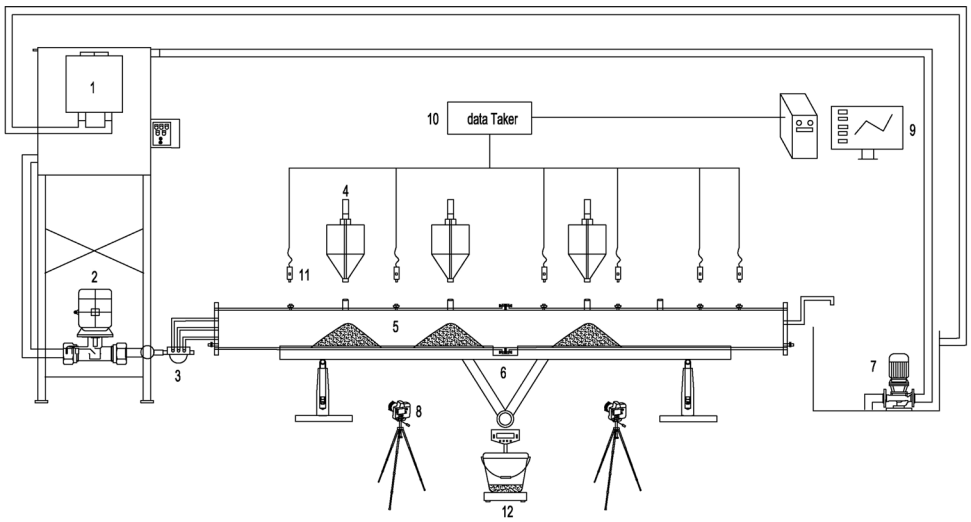

(a) Schematic diagram of the experimental system

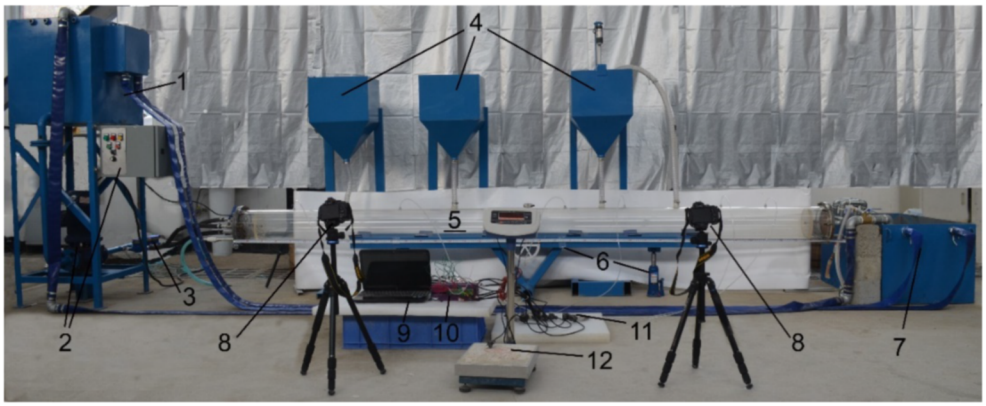

(b) Photo

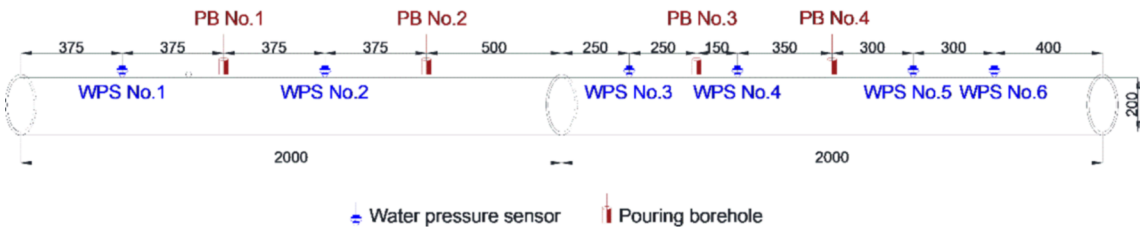

(c) Layout of the boreholes and sensors (units: mm)

Fig. 2 Experimental setup of the aggregate pouring process into an inundated mine tunnel through multiple boreholes under flowing water conditions. 1-water supply with a constant head; 2-water flow rate adjusting device; 3-water meter; 4-funnel for aggregate pouring; 5-tunnel replica; 6-inclination adjuster; 7-water cycling device; 8-camera; 9-PC; 10-data logger; 11-water pressure sensor; 12-electronical balance

The minimum residual water flow channel is the channel with the smallest cross-sectional area for water flow at a certain moment in the pipeline under aggregate accumulation. The minimum residual channel can be formed in two cases, i.e., static and flowing water conditions. The former case occurs due to the existence of the angle of repose resulting in a gap with the tunnel wall, while the latter case can be attributed to the existence of a balance between the resistance of the aggregate particles and the carrying capacity of water flow.

Table 3 Orthogonal array $L_{16}4^5$ for aggregate pouring into a tunnel with water flow

Trial number	Symbol of the trial	Aggregate particle size *A* (mm)	Distance between the boreholes *B* (m)	Initial water flow rate *C* ($\times 10^{-2}$ m/s)	Tunnel inclination *D* (°)	Plugging efficiency *PE* (%)
1	*A1B1C1D1*	0.25–0.5	0.5	0	0	98.15
2	*A1B2C2D2*	0.25–0.5	0.75	1.5	3	94.65
3	*A1B3C3D3*	0.25–0.5	1.0	2.4	5	88.79
4	*A1B4C4D4*	0.25–0.5	1.5	3.0	8	83.96
5	*A2B1C2D3*	0.5–1.0	0.5	1.5	5	94.80
6	*A2B2C1D4*	0.5–1.0	0.75	0	8	97.83
7	*A2B3C4D1*	0.5–1.0	1.0	3.0	0	91.86
8	*A2B4C3D2*	0.5–1.0	1.5	2.4	3	92.65
9	*A3B1C3D4*	1.0–2.0	0.5	2.4	8	93.20
10	*A3B2C4D3*	1.0–2.0	0.75	3.0	5	91.23
11	*A3B3C1D2*	1.0–2.0	1.0	0	3	97.74
12	*A3B4C2D1*	1.0–2.0	1.5	1.5	0	94.94
13	*A4B1C4D2*	2.0–5.0	0.5	3.0	3	96.09
14	*A4B2C3D1*	2.0–5.0	0.75	2.4	0	97.12
15	*A4B3C2D4*	2.0–5.0	1.0	1.5	8	97.19
16	*A4B4C1D3*	2.0–5.0	1.5	0	5	96.27

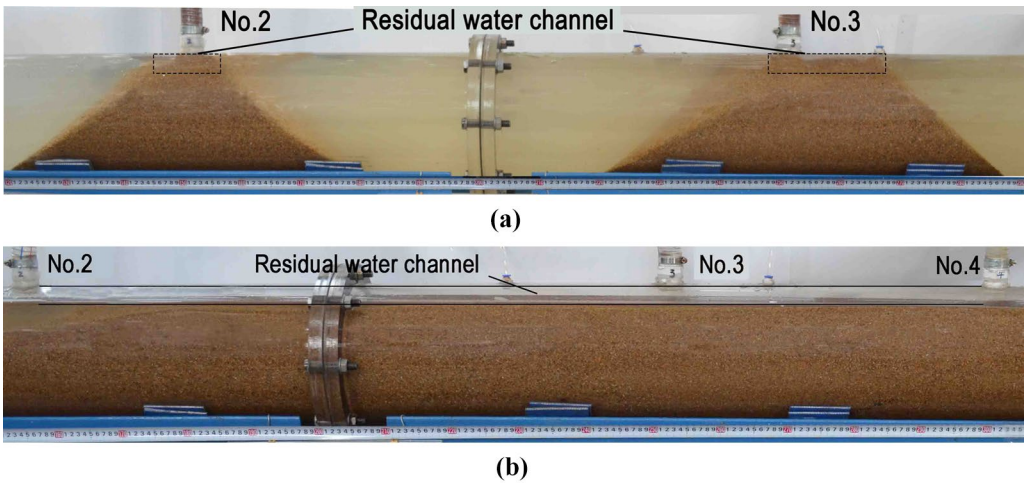

Fig. 3 Minimum residual and final channel under **a** hydrostatic conditions and **b** flowing water conditions

Figure 3a shows a residual channel under static water conditions.

Under flowing water conditions, aggregates could accumulate behind the pouring boreholes because of water flow. Due to friction between the aggregates and pipe wall, at a certain moment, there could occur a minimum water flow channel in the pipe. The surface of the aggregated mass below the channel exhibits a certain curvature with lower values at the middle and higher values on the sides, and eventually, the surface can become horizontal.

The final residual water flow channel is the channel formed between the surface of the sand bed formed after stable accumulation of aggregates in the tunnel and the tunnel wall. With increasing accumulation, a stable sand bed is finally formed comprising sand with a certain particle size after flow rate stabilization. At this time, the surface of the deposited mass below the water flow channel is nearly flat and straight, and the aggregates move as a bedload under the action of water flow. Figure 3b shows a final residual water channel under flowing water conditions.

When the water flow rate near the aggregate accumulation mass in the tunnel remains stable and aggregate pouring continues, the bed sand height remains basically unchanged for a certain time. Therefore, the effect of aggregate plugging remains unchanged. However, water flow can carry aggregates along the roadway toward the front end. With decreasing kinetic energy of the particles, aggregates can accumulate on the sand bed until almost reaching the top and filling the entire cross section (Fig. 3b). The important factors influencing the size and type of the sand bed mass are the water flow rate, aggregate particle size and water flow depth. The smallest residual channel is formed before the final residual channel. At this time, the flow rate is the highest, the channel is usually unstable, and the channel is also the closest to the capping moment. At this time, the pouring amount and aggregate particle size should be increased over time. In the end, a smaller residual channel results in a better plugging effect. When the flow rate in the final residual channel is very high in the test and exceeds the critical velocity of the introduced aggregates, the accumulation mass is continuously pushed forward until the outlet is reached and overflow occurs.

Criterion for the plugging efficiency

The final plugging efficiency (*PE*) is the ratio of the cross-sectional area of the final aggregate accumulation mass to the cross-sectional area of the tunnel.

$$PE(\%) = \frac{P_{\mathrm{f}}}{P_0} \tag{1}$$

where P_{f} is the cross-sectional area of the final aggregate accumulation mass and P_0 is the cross-sectional area of the tunnel, 31,415.93 mm^2.

Figure 4 shows the cross-sectional area of the final aggregate accumulation mass:

$$P_{\mathrm{f}}=\frac{\pi D^2}{4} - \frac{D^2}{8}\left\{\cos^{-1}\left(1-\frac{2H}{D}\right) - \sin\left[\cos^{-1}\left(1-\frac{2H}{D}\right)\right]\right\} \tag{2}$$

where D is the diameter of the tunnel and H is the distance between the aggregate accumulation mass surface and the top of the tunnel; H was measured by photogrammetry of the accumulation masses during pouring.

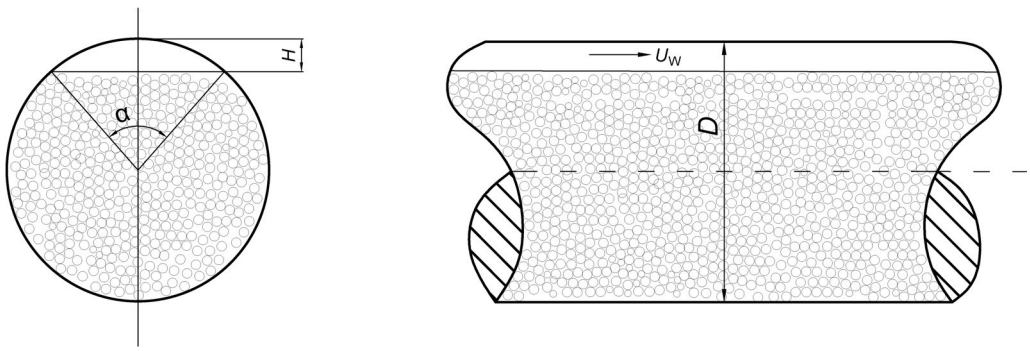

Fig. 4 Cross-sectional area of aggregate deposits in a tunnel

Table 4 Range analysis of the main factors of the plugging efficiency in a tunnel with flowing water

Levels	Aggregate particle size *A* (mm)	Distance between boreholes *B* (m)	Initial water flow rate *C* (10^{-2} m/s)	Tunnel inclination *D* (°)
PE_1	91.39	95.56	97.50	95.52
PE_2	94.29	95.21	95.39	95.28
PE_3	94.28	93.90	92.94	92.77
PE_4	96.67	91.95	90.78	93.05
Range	5.28	3.60	6.71	2.74

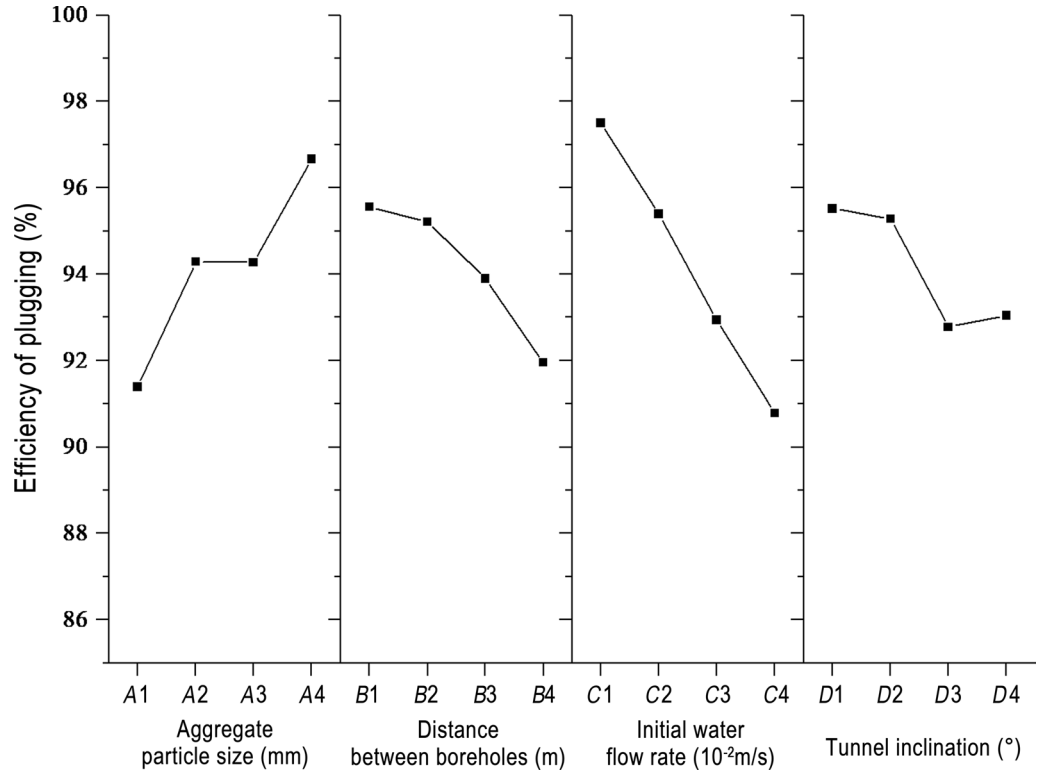

Fig. 5 Response graph for the main factors according to Table 4

Main effects

Range and variance analysis methods are commonly used methods for orthogonal experiments. These experiments can reveal the degree of influence of various factors on the results, primary and secondary orders and optimal combination. Table 3 lists the final plugging efficiency (*PE*).

Range analysis

Table 4 shows the results of range analysis for the different factors, and Fig. 5 shows a response graph.

As the aggregate particle size was increased from *A*1 to *A*4, the plugging efficiency tended to increase. This is related to the critical velocity of the aggregate particles. The accumulation mass of coarse-grained aggregates is rapidly established, and the final height of the accumulation mass is larger than that consisting of fine aggregates. Therefore, with increasing particle size, the plugging efficiency increases. However, under static water conditions, the aggregate accumulation mass exhibits an underwater angle of repose. When the particle size is greater than 0.25 mm, the angle of repose increases with the aggregate particle size, the residual channel area increases, and the plugging efficiency decreases. As the distance between boreholes was increased from *B*1 to *B*4, the plugging efficiency tended to decrease. A smaller distance between boreholes resulted in faster agglomeration of the accumulation masses to form a water blocking section. In addition, the plugging effect was better. As the initial water flow rate was increased from *C*1 to *C*4, the plugging efficiency decreased. Because the water flow rate increased, the ability to carry aggregates increased. The aggregate accumulation mass height hardly increased at a high water flow rate. The larger the residual water channel is, the poorer the water blocking effect. As the tunnel inclination was increased from *D*1 to *D*4, the plugging efficiency exhibited a decreasing trend. The tunnel inclination angle was selected as lower than 10°, which is lower than the friction angle of sand. Therefore, this factor imposed a relatively smaller effect on aggregate settlement and the water blocking effect than that of the other factors.

The result of $R_C > R_A > R_B > R_D$ indicates that the plugging efficiency is influenced by these four factors in the following descending order: initial water flow rate, aggregate particle size, distance between boreholes and tunnel inclination.

Table 5 Variance analysis of the main factors of *PE*

Source of deviation	Deviation sum of squares	Degrees of freedom	Mean square error	*F* ratio	$F_{0.025}$ (3,3) critical value	$F_{0.05}$ (3,3) critical value
Particle size of aggregates *A*	55.99	3	18.66	12.93	15.44	9.28
Distance between boreholes *B*	31.95	3	10.65	7.38	15.44	9.28
Initial water flow rate *C*	102.18	3	34.06	23.59	15.44	9.28
Tunnel inclination *D*	25.04	3	8.35	5.78	15.44	9.28
Error	4.33	3	1.44			

Analysis of variance

Table 5 lists the analysis of variance (ANOVA) results for the factors of the aggregate water blocking effect. The reliability of ANOVA is $1-\alpha$, where α is set to 0.025 and 0.5.

$F_C > F_{0.025(3,3)}$. The initial water flow rate is significant at the level of $\alpha = 0.025$, with a credibility of 0.975. Combined with the range analysis results, it can be found that the initial water flow rate is the most important factor affecting the rate of aggregate plugging. Therefore, the initial water flow rate is the first factor that should be considered in the design of water plugging projects.

$F_A > F_{0.05(3,3)}$. The aggregate particle size is significant at the level of $\alpha = 0.05$, with a credibility of 0.95. Combined with the above range analysis results, it can be observed that the aggregate particle size is second only to the initial water flow rate, so the aggregate particle size notably influences the process of aggregate pouring. The effect of the distance between the boreholes and tunnel inclination on the plugging efficiency is slight.

The above analysis indicates that the factors influencing the plugging efficiency are mainly the initial water flow rate and aggregate particle size, followed by the distance between boreholes and tunnel inclination. The initial water flow rate is not an artificially controllable factor. The results also demonstrate that the optimal combination is *A*4*B*1*C*1*D*1, but this combination was not included in this experiment; the closest combination is *A*1*B*1*C*1*D*1. In actual engineering, we should choose the remaining three factors of the aggregate particle size, distance between boreholes and tunnel inclination (or location) to achieve the best water plugging effect.

Interaction between factors

Aggregate particle size and distance between boreholes

The two factors of the aggregate particle size and distance between boreholes can be artificially selected in actual engineering, and the experimental results indicate that there exists interaction between these two factors. Figure 6a shows that there are two regions of a high plugging efficiency. The first one in the left lower part suggests that the smaller the aggregate particle size (0.25–0.5 mm) and the distance between boreholes (0.5–0.75 m) are, the higher the plugging efficiency, i.e., a fine aggregate particle size should be used in the case of a small drilling spacing. The second one is located in the right and upper parts. This region indicates that a good plugging efficiency can be obtained for intermediate particle sizes (0.75–1.5 mm) in the case of a large borehole spacing. For larger particle sizes (2–5 mm), the overall plugging efficiency is high, and the influence of the borehole spacing decreases. The main reason for the formation of these two regions is the interaction between gravity and drag forces. Regarding fine aggregates, the accumulation process is slow due to low gravity forces, and multiple boreholes pouring with a small spacing can easily and quickly form a continuous accumulation mass. Given a small borehole spacing, an accumulation mass can easily form, and the residual water channel is smaller. However, the accumulation mass can be easily washed away at a high water flow rate. In contrast, the gravity forces of coarse particles are higher, and the deposition process in water occurs fast, resulting in a long continuous accumulation mass in the aggregate pouring process involving multiple boreholes with a larger spacing.

In actual engineering, fine aggregates should be poured under a small borehole spacing. Coarser aggregates should be poured via more widely spaced boreholes or at certain intervals. At the same time, when selecting the distance between boreholes, consideration should be given to reducing the influence of water turbulence on the pouring process to quickly form a bulk mass.

Aggregate particle size and initial water flow rate

Aggregates of different particle sizes achieve unique critical velocities, and it is important to choose aggregates of an appropriate particle size to realize fast aggregate accumulation and deposition and water blocking in a given tunnel. Figure 6b shows that when the initial water flow rate ranges from 2×10^{-2} to 3×10^{-2} m/s, the plugging efficiency is proportional to the aggregate particle size, and coarser aggregates can yield a better plugging effect. When the initial water flow speed is lower than 2×10^{-2} m/s, aggregates with a particle size smaller than

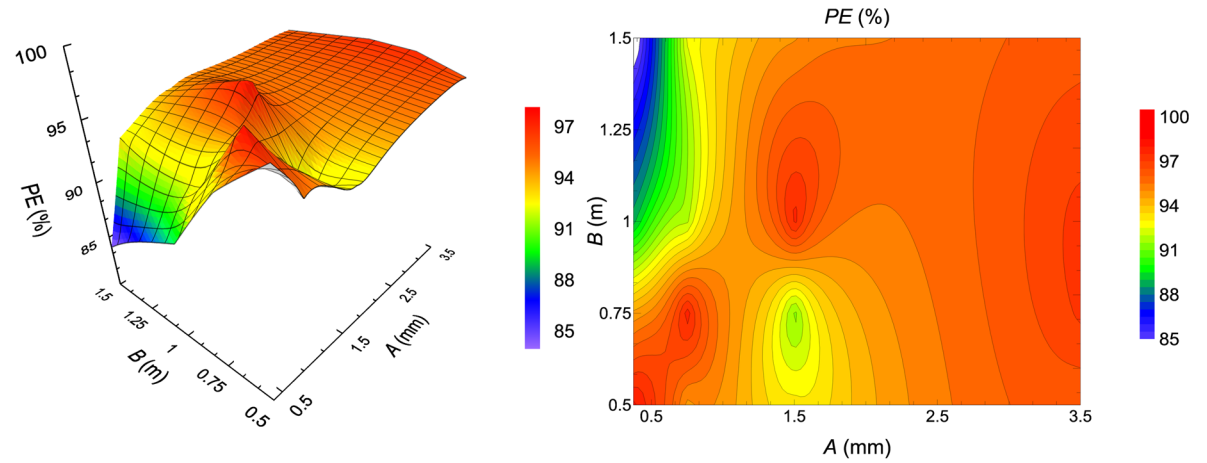

(a) Aggregate particle size A and distance between boreholes B

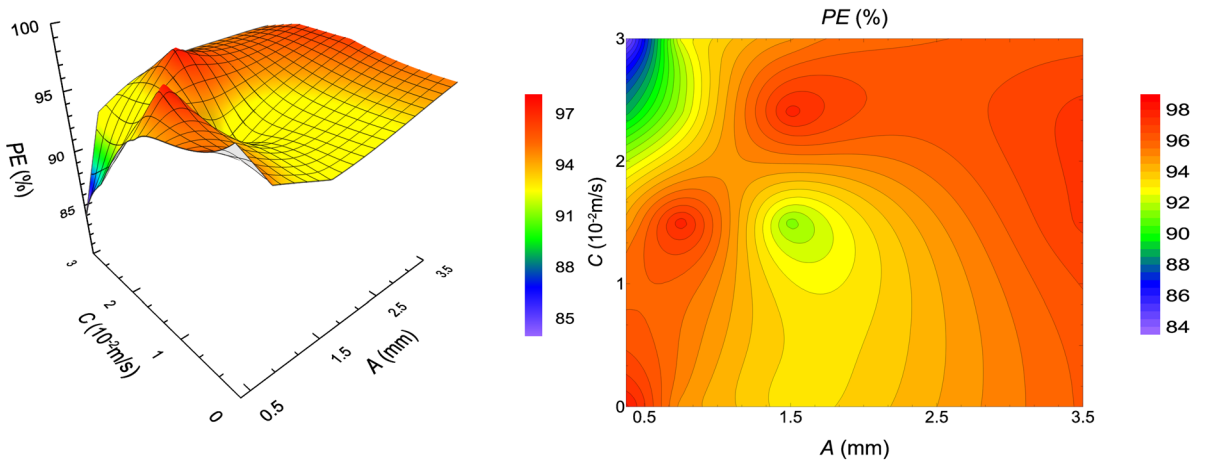

(b) Aggregate particle size A and initial water flow rate C

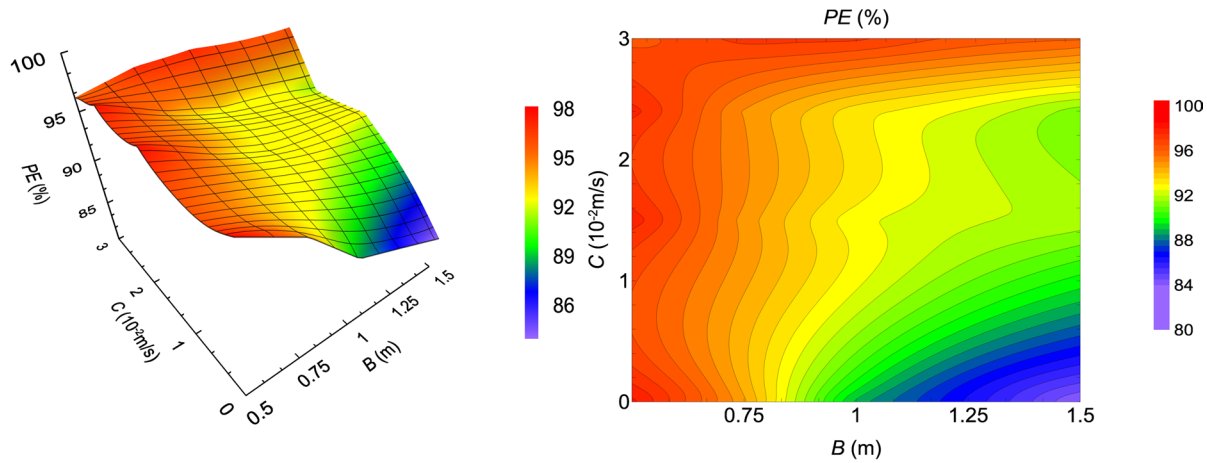

(c) Distance between boreholes B and initial water flow rate C

Fig. 6 *PE* under various combinations of the different factors

0.5 mm can provide the best plugging effect. When the aggregate particle size varies between 1 and 2 mm, the plugging efficiency is lower than that achieved with the other aggregate particle sizes. The plugging efficiency for the different aggregate particle sizes is more greatly affected by the initial water flow rate, which does not suggest that the aggregate particle size determines the final effect. In actual engineering, it is necessary to choose an appropriate particle size for different initial water flow rates.

Distance between boreholes and initial water flow rate

According to the Reynolds criterion, turbulence is more likely to occur at a high flow rate when the cross section and characteristic length of the tunnel are fixed. It was found that the turbulence due to water flow restricted the pouring speed, and the turbulence exhibited a certain relationship with the initial water flow rate. Considering that the flow velocity of moving water is relatively high in actual projects, it is meaningful to choose a suitable distance between boreholes. Figure 6c shows that the influence of the initial water flow rate on the plugging efficiency is very obvious, and the initial water flow rate exerts a greater influence than that of the distance between boreholes. When the initial water flow rate is low and the distance between boreholes is smaller than 0.75 m, a higher plugging efficiency can be obtained (red area). The plugging efficiency is low when the distance between boreholes ranges from 0.75 to 1.5 m. When the distance between boreholes is small, the turbulence more significantly affects the pouring process, and boreholes can become severely blocked. When the initial water flow rate is higher than 2.4×10^{-2} m/s, the influence of the distance between boreholes on *PE* is relatively limited. The contour of high *PE* values is biased toward the direction of a higher initial water flow rate.

Water pressure during plugging

The layout of water pressure sensors is shown in Fig. 2c. The water pressure measurements during the pouring process reveal that there exists a pressure difference between the front and back ends of the formed aggregate accumulation mass. Even if the aggregate accumulation mass has not been capped, water flow can still be greatly impeded if a certain length is reached.

Figure 7a shows changes in the water pressure in the tunnel in Trial No. 2. In the figure, t_0 is the time to start pouring, t_1 is the time to end pouring from funnel No. 2, t_2 is the time to end pouring from funnel No. 1, and t_{final} is the time when the accumulation mass form has stabilized. Before the start of pouring, due to friction between the wall and water flow, the pressure in

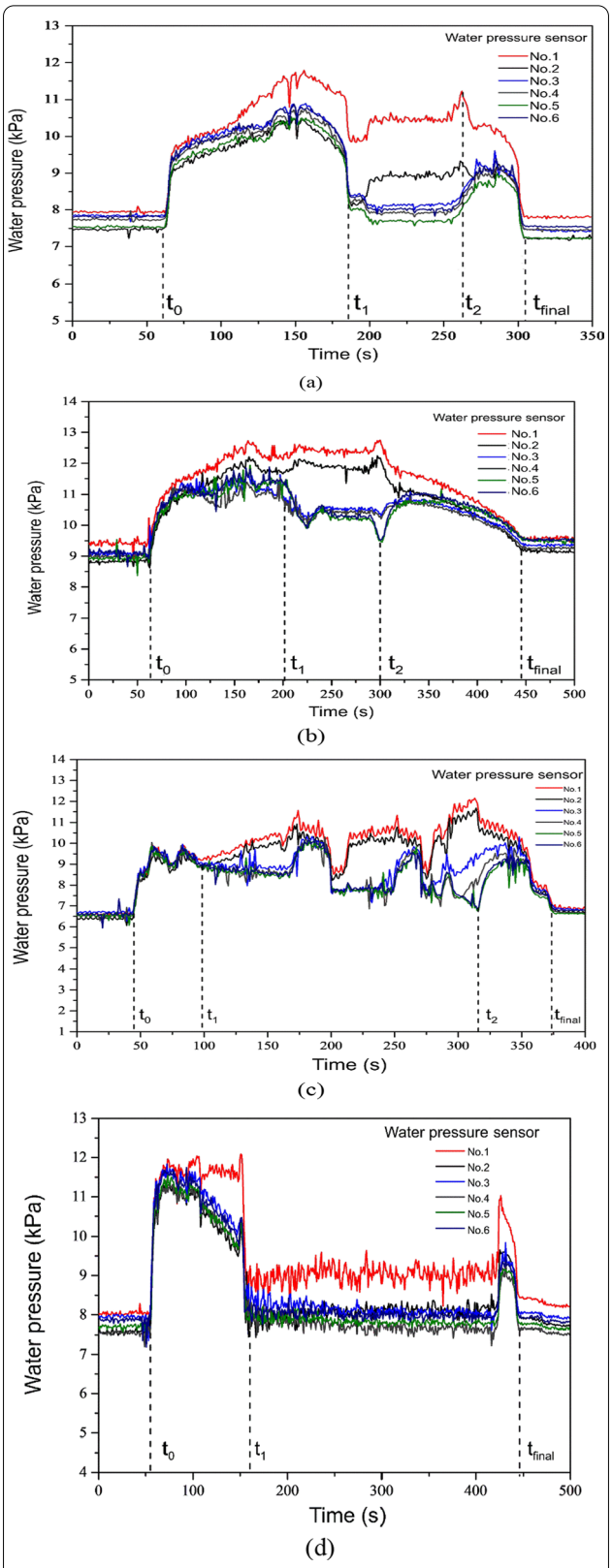

Fig. 7 Water pressures during aggregate pouring in **a** Trials No. 2; **b** No. 3; **c** No. 12; and **d** No. 14

the tunnel can be reduced along the flow direction. The pressures measured by the six pressure sensors gradually decrease, but the difference is small. At time t_0, the water pressure in the tunnel instantaneously rises because the water–sand mixture in the funnel reaches inside the tunnel and becomes connected with the tunnel. As pouring proceeds, the accumulation masses below the two boreholes become connected, and the pressure at pressure sensor No. 1 rises faster than that at the other sensors. This indicates that the aggregate accumulation mass has contacted the top of the tunnel and that the resistance to water flow has increased. Then, at time t_1, the pressure suddenly drops because pouring stops in borehole No. 2 and the water pressure originating from the funnel drops. Afterward, as pouring is continued in borehole No. 1, the pressure at sensors No. 1 and No. 2 begins to rise to a stable value, and the pressure at sensors No. 3, 4 and 5 falls, resulting in a large pressure difference between the front and back ends of the accumulation mass. At time t_2, the pouring process in borehole No. 1 stops, and the pressure finally drops. At this time, the smallest residual channel is gradually stabilized by the water flow. At time t_{final}, the final residual channel is formed, and the water pressure in the tunnel eventually matches the initial pressure before pouring.

The water pressure changes in the other trials, as shown in Fig. 7b, c and d, are relatively similar to those in this trial. The energy source of aggregate movement in the tunnel is the potential energy of water flow (or pressure difference), kinetic energy of the internal turbulence and potential energy of the aggregate particles. A change in water pressure reflects the water head loss, and a large pressure difference varying between 16.0% and 31.8% occurs before and after accumulation mass stabilization (from time t_1 to t_2) in the tunnel. In the case of the same particle size, the faster the water flow is, the smaller the pressure difference. Even if the aggregate accumulation mass is not capped, under the premise of continuous pouring, the aggregate accumulation mass still provides a suitable resistance effect on water flow.

Discussion

Sedimentation of aggregates

Shape of the aggregate accumulation mass

The sand and water used in this experiment were mixed according to a water–solid mass ratio of 1:1–2:1, and the two boreholes were filled simultaneously. Figure 8 shows the final shape of the aggregate accumulation mass. The extension of the accumulation mass along the direction of water flow can be mainly divided into three segments: an accumulation mass on the front surface, an accumulation mass on the back surface and an accumulation mass between the holes. The details for this division are described in the literature (Zhang et al. 2020). The shape of the accumulation mass between the boreholes when capped is controlled by the shape of the tunnel. The larger the aggregate particle size is, the steeper the edge of the accumulation mass. Aggregate particles are subjected to a water flow impulse on the water-facing surface, and the accumulation mass occurs in convex contact with the tunnel wall on the upstream side and in concave contact on the downstream side. An obvious difference in the accumulation mass shape in the experiments is mainly manifested upon a reduction in aggregate particle size,

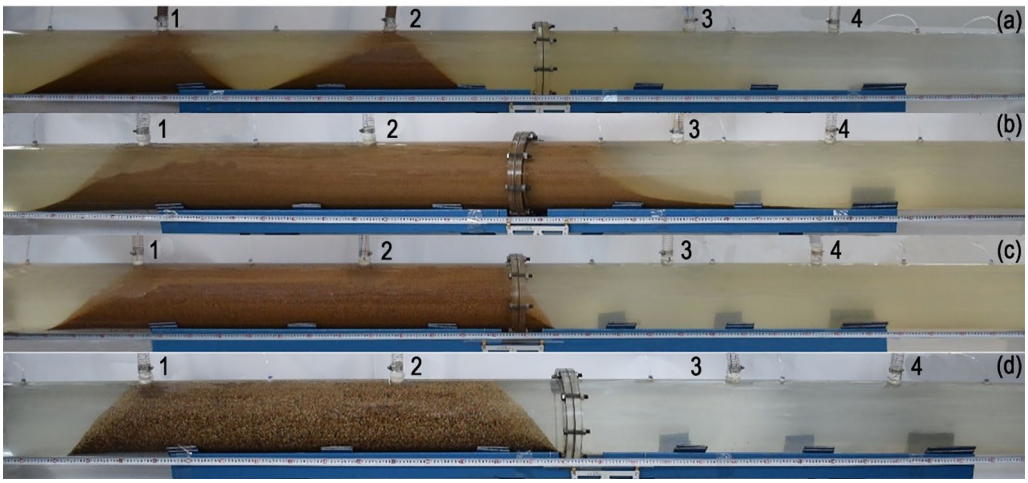

Fig. 8 Aggregate accumulation mass in **a** Trial No. 6 ($A=0.5$–1 mm, $B=0.75$ m, $C=0$, and $D=8°$); **b** Trial No. 2 ($A=0.25$–0.5 mm, $B=0.75$ m, $C=1.5\times10^{-2}$ m/s, and $D=3°$); **c** Trial No. 10 ($A=1$–2 mm, $B=0.75$ m, $C=3\times10^{-2}$ m/s, and $D=5°$) and **d** Trial No. 14 ($A=2$–5 mm, $B=0.75$ m, $C=2.4\times10^{-2}$ m/s, and $D=0°$)

increase in the water flow rate, increase in tunnel inclination and increase in pouring volume. In particular, there is a notable difference in the shape of the aggregate accumulation mass between static and flowing water conditions in the tunnel.

Figure 8a shows the shape of the sand aggregate accumulation mass in an 8° inclined tunnel under static water conditions. The aggregate settlement is similar to that under free sedimentation in a river under steady-state flow. Under gravity, buoyancy, drag and other forces, aggregates accelerate at a certain initial speed, settle at the bottom of the tunnel, and are quickly capped. When the aggregates contact the top wall of the tunnel, they do not easily settle, particularly coarse particles, so the borehole can easily become plugged. In horizontal pipes, the accumulation masses below the two boreholes are basically symmetrical on the left and right sides of the holes. With a smaller distance between boreholes and finer aggregates, the accumulation masses can be quickly connected to form a section with a suitable water plugging effect, for instance, in Trial No. 1. However, under a large distance between boreholes, there occur two separate accumulation masses in the inclined tunnel that are similar to an asymmetrical cone shape (Fig. 8a). The larger the angle and the smaller the particle size are, the more obvious the difference between the two sides of the accumulation mass. Under static water conditions, the particle size generates an underwater friction angle (angle of repose). To continuously move the aggregates along the horizontal direction, the impact force caused by pouring must be greater than the shear strength of the aggregate accumulation mass with a certain shape. The accumulation masses become connected to form a water blocking section with a certain length. Therefore, reasonable selection of the distance between boreholes and aggregate particle size is very important. The contact conditions of the aggregate accumulation masses in static water within the tunnel are not very stable. When a certain water flow rate is applied, the particles at the top of the aggregate accumulation mass move. In this case, the pouring speed or aggregate particle size should be adjusted to form a blocking section that is appropriate for further grouting reinforcement.

Figure 8b, c, and d show the accumulation patterns for three aggregate particle sizes under flowing water conditions, at tunnel inclinations of 3°, 5° and 0°, respectively. The factors influencing the accumulation and distribution of aggregates in flowing water are more complex than those in static water. The forces include gravity, lifting, drag, interparticle, and seepage forces. The state of water flow and movement of sand particles in flowing water should be considered in particle accumulation. Before the aggregate mass reaches its maximum height for the first time, particles mainly accumulate under vertical settlement. When the water flow rate increases close to the critical condition of particle movement, the particles begin to move mainly along the direction of water flow, and the accumulation masses slowly become connected. When the initial water flow rate is high, the critical condition of particles is easily reached, and the time for the aggregates to settle is shortened. The maximum height of the aggregate accumulation mass is smaller than that under a low flow rate. Under the same conditions, the remaining water passages are larger, and the water blocking effect is poorer. The critical flow rate for coarse particles is higher than that for fine particles. The height of the coarse sand accumulation mass is larger than that of the fine sand accumulation mass. Coarse sand extends less along the direction of water flow than does fine sand.

Gravity component forces alter the shape of the aggregate accumulation mass in an inclined tunnel. The larger the angle is, the more obvious the difference in the morphology of the accumulation mass between both sides of the pouring borehole.

Process of plugging

Figure 9a shows the accumulation process of aggregates with a particle size ranging from 2 to 5 mm in static water in Trial No. 6. In a tunnel inclined at 8° under static water conditions, a mixture of water and fine sand enters the tunnel at a certain initial water flow rate. Under the action of gravity and drag forces in the water flow, the aggregates are scattered at the bottom of the tunnel. Over time, the settlement process continues to intensify beneath the borehole, and aggregate settlement is biased toward low-lying locations in the tunnel, with increased extension. It is found that coarse sand accumulates faster than do fine particles. The pouring speed in borehole No. 2 is relatively high, so the aggregate accumulation mass below this borehole is formed faster.

Figure 9b shows that a coarse sand-water mixture enters a horizontal tunnel under flowing water conditions at a certain initial rate. The instantaneous initial speed of pouring is much higher than the water flow rate inside the tunnel; thus, the aggregates settle quickly. However, with increasing height of the accumulation mass, the size of the water flow channel decreases, and the water flow rate continues to increase until it is higher than the startup critical velocity of the particles. Therefore, particles are carried forward by the water flow and mainly settle on the downstream side of the accumulation mass under bedload conditions, and fewer sand

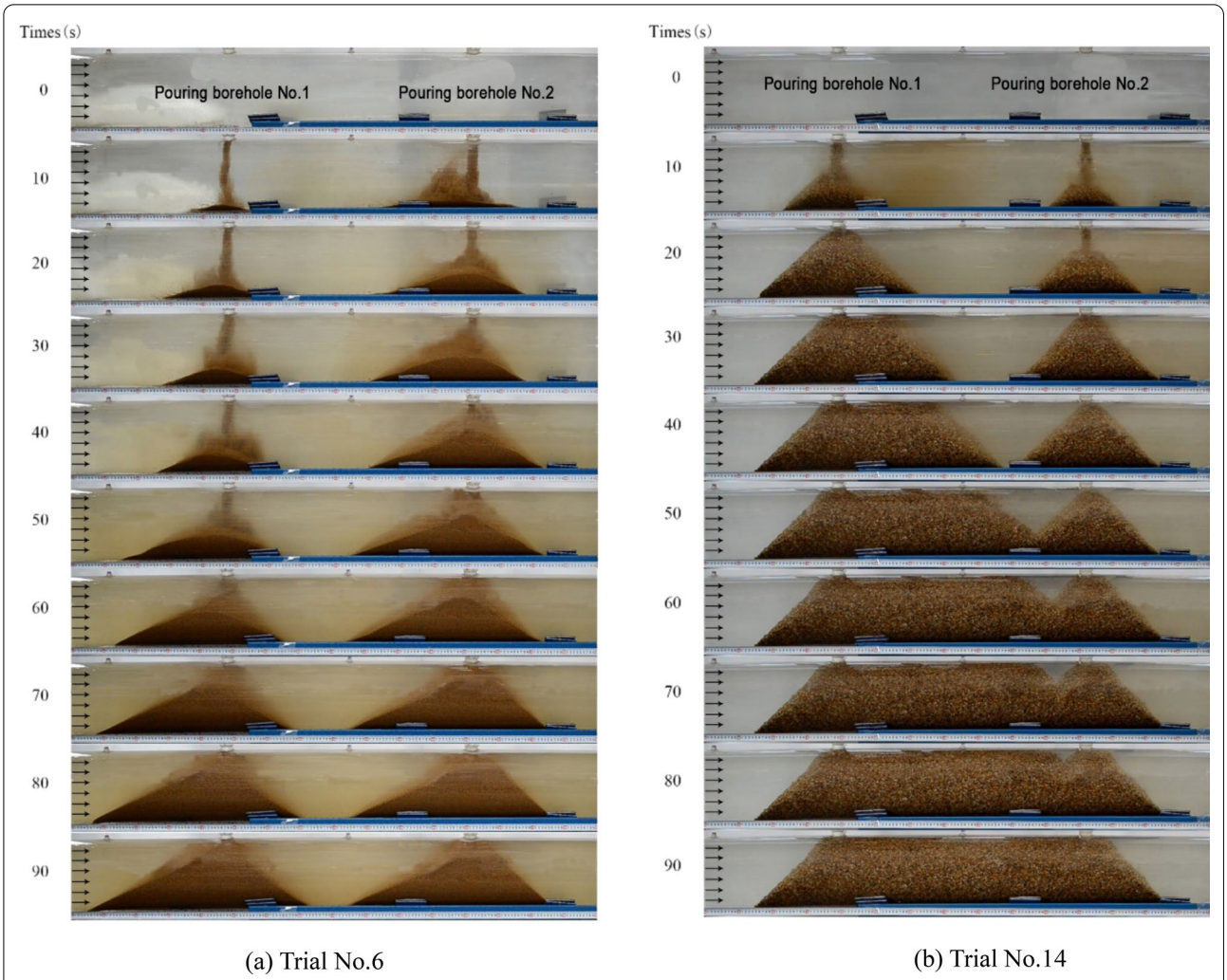

Fig. 9 Plugging process of aggregates (the arrows indicate water flow)

particles settle on the side upstream. However, when the aggregate mass approaches its maximum height for the first time, the water flow becomes highly turbulent. The water flow accelerates at the front and decelerates at the back. Due to the sudden change in flow velocity, the pressures in the upper and lower parts of the back side of the accumulation mass below borehole No. 1 are inconsistent. A circulation current occurs, which is similar to flow around a cylinder in hydrodynamics. Where the residual channel is small, the water flow is turbulent, and trailing vortices occur. For example, vortices can be clearly observed in Trials No. 2 and No. 3. The finer the particles are, the more severe the disturbance of the sand-carrying water flow, and the more particles in the suspended mass are deposited on the back side of the accumulation mass. Under downstream extension, the space between the two masses is continuously filled, which eventually produces a water blocking section. For example, in Trial No. 14, aggregates filled the tunnel continuously until the space between the two boreholes was completely eliminated (Fig. 9b).

Under the condition of the same distance between boreholes, the required amount and time for aggregate pouring are the issues to be considered in the rapid construction of the aggregate accumulation mass. Connecting the accumulation masses between the boreholes during the shortest time with the minimum injection volume is important for plugging section construction. As indicated above, coarse particles more easily and more rapidly produce accumulation masses than do fine particles. However, the water pressure difference between the front and back ends of the accumulation mass is more notable for finer particles than for coarse particles under the same distance between boreholes. The greater the water head loss, the easier it

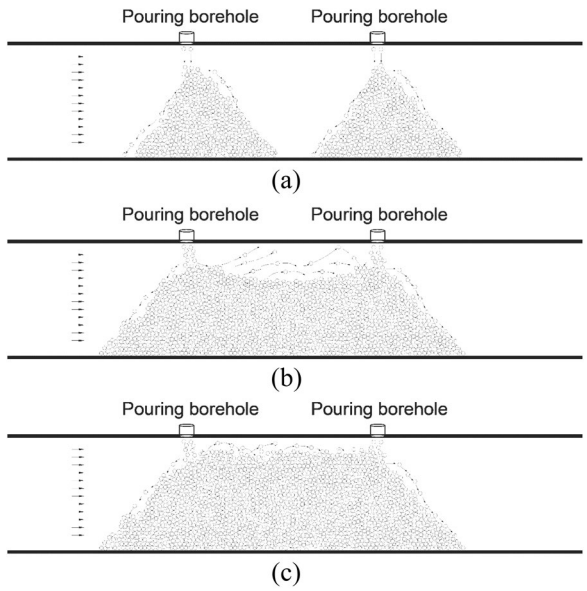

Fig. 10 Aggregate movement at the different stages of the establishment of the water-blocking section. **a** Settlement and accumulation stage; **b** Connection and accumulation stage; **c** Capping and accumulation stage

is for the aggregate mass to become capped. Therefore, a reasonable combination of fine and coarse particles is the key to the rapid construction of the water-blocking section.

Movement and deposition of aggregates

The movement pattern of pipeline sand particles in this test can be roughly divided into three stages based on the three stages reported in the literature (Wang 2012).

The first stage is denoted as the settlement and accumulation stage. Figure 10a shows that the aggregates quickly and vertically accumulate before reaching the top for the first time. The cross-sectional area of the water channel decreases, the particles mainly move as a cohesive mass, and very few particles move as suspended particles.

The second stage is the connection accumulation stage. As shown in Fig. 10b, the accumulation mass reaches its maximum height for the first time, namely, the water flow carrying capacity is higher than the critical condition for particle movement. At this time, the water flow is turbulent and accompanied by vortices. The settling particles move in the form of bed and suspended masses under the action of turbulent water flow and vortices. The bed mass includes contact and jumping masses, which settle downstream. The accumulation mass extends forward and finally is connected into a whole.

The third stage is defined as the capping and accumulation stage. As shown in Fig. 10c, the aggregate accumulation mass in the tunnel is similar to that on a static riverbed. The introduced aggregates move mainly in the form of a bedload and some suspended matter in the residual channel at the top of the accumulation mass. The aggregates are deposited on the back side of the entire accumulation mass. After reaching a certain length, the sand-carrying capacity of the water flow cannot move the mass. The particles are mainly dominated by contact and jumping movements. The aggregates continue to accumulate. A stable water blocking segment can eventually be formed.

Plugging criterion

The water-blocking section of an accumulation mass formed via aggregate pouring in a concentrated waterway initially resists water flow impulses and reduces the water flow intensity. At this time, there is still much seepage in the water-blocking section, facing the danger of being washed away by water at any time. It is necessary to implement grouting. Therefore, the aggregate plugging criterion is of great importance to determine the timing of grouting. The above force balance analysis and plugging efficiency can be used as plugging criteria in experiments and projects. In practical engineering, the plugging criterion can be summarized as (Guo 2005): (1) the top interface of the aggregates in the borehole should be higher than the elevation of the tunnel. After sweeping the borehole bottom, the poured aggregates hardly settle, and the height of the accumulation mass is higher than the top of the water channel. (2) The water-blocking section can resist water flow. There exists a large constant water level difference between the front and back ends of the water-blocking section, and the friction between the water-blocking section and tunnel wall can resist water flow impulses, ensuring that this section is not washed away in a short time. (3) The unit water injection is lower than 16×10^{-3} m^3/min·m. Usually, all the above criteria are met to determine that a stable water-blocking section is built. At the same time, a critical condition for the movement of particles in a horizontal or an inclined tunnel can be used to evaluate the stability of aggregates (Zhang et al. 2020).

Limitations and further study

The injection speed in the aggregate pouring process in this experiment is different from the actual speed. The pouring speed affects the porosity and other properties of the aggregate accumulation mass. The angle of

the tunnel selected in this study is very low. When the tunnel inclination is greater than the angle of repose of the aggregate accumulation mass, there are certain changes. It is therefore meaningful to study the influence of the injection speed, sequence of aggregate pouring, and mixing of different particle sizes on the plugging effect. Generally, the actual tunnel cross section is not circular. The sedimentation and migration processes of particles in different cross-sectional shapes will vary. In the next step, a cross-sectional shape closer to that in actual projects will be selected during aggregate pouring into a large-passage tunnel. In addition, the pressure in this test is low. Certain properties of high-pressure water flow can influence aggregate accumulation, including the state, density, and permeability. In actual projects, the water pressure reaches higher than 3 MPa. Further research should be conducted to investigate the effect of high-pressure water flow on the properties of aggregate accumulation. Another limitation is that the model wall is relatively smooth, and the roughness is not considered. A follow-up study should focus on the effect of different roughnesses on the blocking effect of the aggregate accumulation mass under the premise of ensuring visualization.

Conclusions

An experimental investigation on the plugging effects of aggregate pouring through multiple boreholes under flowing water conditions in an inundated tunnel was conducted, and the results were examined in this paper.

A visual test platform for aggregate pouring into a tunnel was built. This platform could realize the visualization of the aggregate pouring process into the tunnel under multiple factors and levels and realize real-time collection of image, pressure and flow data.

A four-level orthogonal array experimental test was performed. Range and variance analysis of the results indicated that the factors controlling the plugging efficiency are the initial water flow velocity, aggregate particle size, distance between boreholes and tunnel inclination in descending order.

The shape of the aggregate deposit mass was analyzed, and the results revealed that the extension of the accumulation mass along the direction of water flow could be mainly divided into accumulation masses at the front, at the back and between the boreholes. The shape of the accumulation mass between the boreholes was similar to the shape of the tunnel when capped. The shape of the aggregate accumulation mass is quite different between static and flowing water conditions.

The measured water pressure difference between the front and back ends of the formed aggregate mass during the pouring process indicates that the water flow is greatly restricted, even if the aggregate mass is not capped but reaches a certain length.

The critical condition for particle sedimentation and accumulation is that the equilibrium state of the resultant forces should reach zero before the deceleration motion of the particles. A plugging criterion for aggregate deposition in horizontal and inclined tunnels was proposed. Moreover, it was proposed that the minimum plugging length of the aggregate deposit should be greater than the theoretical minimum length of effective grouting. When the aggregate pouring boreholes are not influenced by each other, a small spacing between boreholes should be selected.

Acknowledgements
The authors thank the Natural Science Foundation of China for the provided support under Grant No. 41877238.

Author contributions
WS and GZ proposed the main idea of this study and designed the experiments. SH performed the experiments and analyzed the results. JC and SY performed the field investigation and edited and wrote part of the paper. All authors have read and approved the final manuscript.

Funding
This study was supported by the Natural Science Foundation of China under Grant No. 41877238.

Availability of data and materials
All data generated or analyzed in this study are included in the published article.

Declarations

Competing interests
The authors declare that they have no competing interests.

Author details
[1]School of Resources and Geosciences, Institute of Mine Water Hazard Prevention and Control Technology, China University of Mining and Technology, Xuzhou 221116, China. [2]China Design Group Co., Ltd., Nanjing 210014, China. [3]National Coal Mine Water Hazard Prevention Engineering Technology Research Center, Suzhou 234000, Anhui, China. [4]Institute of Mining Engineering Research and Design, BGRIMMM Technology Group, Beijing 100160, China.

Received: 4 February 2022 Accepted: 25 June 2022
Published online: 07 July 2022

References

Allahvirdizadeh P, Kuru E, Parlaktuna M (2016) Experimental investigation of solids transport in horizontal concentric annuli using water and drag reducing polymer-based fluids. J Nat Gas Sci Eng 35:1070–1078. https://doi.org/10.1016/j.jngse.2016.09.052

Arolla SK, Desjardins O (2015) Transport modeling of sedimenting particles in a turbulent pipe flow using Euler–Lagrange large eddy simulation. Int J Multiph Flow 75:1–11. https://doi.org/10.1016/j.ijmultiphaseflow.2015.04.010

Bratland O (2010) Pipe flow 2: multi-phase flow assurance. Springer, New York, pp 235–243

Capecelatro J, Desjardins O (2013) Eulerian–Lagrangian modeling of turbulent liquid–solid slurries in horizontal pipes. Int J Multiph Flow 55:64–79. https://doi.org/10.1016/j.ijmultiphaseflow.2013.04.006

Chanson H (2008) Turbulent air–water flows in hydraulic structures: dynamic similarity and scale effects. Environ Fluid Mech 9:125–142. https://doi.org/10.1007/s10652-008-9078-3
Corredor FER, Bizhani M, Kuru E (2016) Experimental investigation of cuttings bed erosion in horizontal wells using water and drag reducing fluids. J Pet Sci Eng 147:129–142. https://doi.org/10.1016/j.petrol.2016.05.013
Dong S, Yang Z, Zhu M, Zhang W, Shi L, Mu L (2020) Development of large-scale simulation experiment system for dynamic water rapid sealing in flowing water roadway. J China Coal Soc 45(9):3226–3235
Duckworth RA, Argyros G (1972) Influence of density ratio on the pressure gradient in pipes conveying suspensions of solids in liquids. In: Proceedings of hydrotransport 2. The 2nd international conference on the hydraulic transport of solids in pipes. BHRA Fluid Engineering, New York
Durand R (1952) The hydraulic transportation of coal and other materials in pipes. Colloquium of National Coal Board, London
Ekambara K, Sanders RS, Nandakumar K, Masliyah JH (2009) Hydrodynamic simulation of horizontal slurry pipeline flow using ANSYS-CFX. Ind Eng Chem Res 48:8159–8171. https://doi.org/10.1021/ie801505z
Fei XJ (1994) Hydraulics of slurry and granular material transport. Tsinghua University Press, Beijing
Graf WH, Robinson M, Yucel O (1970) The critical deposit velocity for solid-liquid mixtures. In: Proceedings of 1st international conference on the hydraulic transport of solids in pipes. BHRA Fluid Engineering, Cranfield
Guo Q (2005) Technology for rapid treatment of major coal mine water hazards: practice and knowledge of grouting to block water. Coal Industry Press, Beijing
Hedayat AS, Sloane NJA, Stufken J (1999) Orthogonal arrays: theory and applications. Springer Science & Business Media LLC, New York
Ji Z (2014) Grouting and water blocking technology under complex conditions of water inrush in coal mine. Explor Eng (Rock Soil Drill Tunnel) 41(5):61–65
Jiang Q (2009) Comprehensive construction technology of water-blocking bulkhead in the with concentrated water flow. Coal Mine Saf 40(5):37–39
Jiang X, Hui S, Sui W, Shi Z, Wang J (2020) Influence of the aggregate-pouring sequence on the efficiency of plugging inundated tunnels through drilling ground boreholes. Water 12:2698. https://doi.org/10.3390/w1206176
Kaushal D, Thinglas T, Tomita Y, Kuchii S, Tsukamoto H (2012) CFD modeling for pipeline flow of fine particles at high concentration. Int J Multiph Flow 43:85–100. https://doi.org/10.1016/j.ijmultiphaseflow.2012.03.005
Kim C, Lee M, Han C (2008) Hydraulic transport of sand-water mixtures in pipelines part I. Experiment. J Mech Sci Technol 22:2534–2541. https://doi.org/10.1007/s12206-008-0811-0
Li CH (2010) Plugging technology for super giant water inrush laneway in mine. J Xi'an Univ Sci Technol 30(3):305–308
Messa GV, Malavasi S (2015) Improvements in the numerical prediction of fully-suspended slurry flow in horizontal pipes. Powder Technol 270:358–367. https://doi.org/10.1016/j.powtec.2014.10.027
Messa GV, Matoušek V (2020) Analysis and discussion of two fluid modelling of pipe flow of fully suspended slurry. Powder Technol 360:747–768. https://doi.org/10.1016/j.powtec.2019.09.017
Messa GV, Malin MR, Malavasi S (2014) Numerical prediction of fully-suspended slurry flow in horizontal pipes. Powder Technol 256:61–70. https://doi.org/10.1016/j.powtec.2014.02.005
Miedema SA (2015) A head loss model for slurry transport in the heterogeneous regime. Ocean Eng 106:360–370. https://doi.org/10.1016/j.oceaneng.2015.07.015
Miedema SA (2016) The heterogeneous to homogeneous transition for slurry flow in pipes. Ocean Eng 123:422–431. https://doi.org/10.1016/j.oceaneng.2016.07.031
Mou L, Dong S, Zhou W, Wang W, Li A, Shi Z (2020) Data analysis and key parameters of typical water hazard control engineering in coal mines of China. Mine Water Environ 39:331–344. https://doi.org/10.1007/s10230-020-00684-9
Mou L (2021) Study on construction mechanism and key technology of water-blocking wall in hydrodynamic pathway. Dissertation, Xi'an Coal Research Institute
Newitt DM, Richardson JF, Abbott M, Turtle RB (1955) Hydraulic conveying of solids in horizontal pipes. Trans Inst Chem Eng 33:93–110
Ni JR, Wang GQ, Zhang HW (1989) Basic theory of two-phase flow and its latest application. Beijing Science Press, Beijing
Pinto TS, Júnior DDM, Slatter P, Filho LL (2014) Modelling the critical velocity for heterogeneous flow of mineral slurries. Int J Multiph Flow 65:31–37. https://doi.org/10.1016/j.ijmultiphaseflow.2014.05.013
Shao H, Wang W (2011) Double liquid grouting method for rapid construction of water blocking bulkhead to block water inrush roadway. Coal Mine Saf 42(11):40–43
Soepyan FB, Cremaschi S, Sarica C, Subramani HJ, Kouba GE (2013) Solids transport models comparison and fine-tuning for horizontal, low concentration flow in single-phase carrier fluid. AIChE J 60:76–122. https://doi.org/10.1002/aic.14255
Thomas A (1979) Predicting the deposit velocity for horizontal turbulent pipe flow of slurries. Int J Multiph Flow 5:113–129. https://doi.org/10.1016/0301-9322(79)90040-5
Turian RM, Yuan T-F (1977) Flow of slurries in pipelines. AIChE J 23:232–243. https://doi.org/10.1002/aic.690230305
Turian RM, Yuan T-F, Mauri G (1971) Pressure drop correlation for pipeline flow of solid-liquid suspensions. AIChE J 17:809–817. https://doi.org/10.1002/aic.690170409
Uzi A, Levy A (2018) Flow characteristics of coarse particles in horizontal hydraulic conveying. Powder Technol 326:302–321. https://doi.org/10.1016/j.powtec.2017.11.067
Vlasák P, Kysela B, Chara Z (2012) Flow structure of coarse-grained slurry in a horizontal pipe. J Hydrol Hydromech 60:115–124. https://doi.org/10.2478/v10098-012-0010-7
Wang W, Hu B (2011) A new technology of rapid sealing roadway in the Luotuoshan coal mine. Proc Earth Planet Sci 3:429–434
Wang S, Wei Z, Lei F, Xue G, Tong X, Li Y (2013) Study on coalmine hidden extraordinary water bursting channel instant sealing technology. China Coal Geol 25(11):31–35
Wang W (2012) Study on techniques of roadway-blocking & flow-cutting off under hydrodynamic conditions and capability evaluation of water-blocking segment. Dissertation, Beijing Coal Science Research Institute
Wasp EJ, Kenny JP, Gandhi RL (1977) Solid-liquid flow: slurry pipeline transportation. Trans Tech Publications, Clausthal-Zellerfeld
Wasp EJ, Slatter PT (2004) Deposition velocities for small particles in large pipes. In: Proceedings of the 12th international conference on transport and sedimentation of solid particles, Prague, Czech Republic, pp 20–24
Wilson KC (1979) Deposition-limit nomograms for particles of various densities in pipeline flow. In: Proceedings of the hydrotransport 6, BHRA Fluid engineering, Cranfield, pp 1–12
Yalin MS (1971) Principles of the theory of similarity. In: Theory of hydraulic models. Macmillan civil engineering hydraulics. Palgrave, London. pp 35–50. https://doi.org/10.1007/978-1-349-00245-0_2
Zhang G, Hui S, Li W, Sui W (2020) Experimental investigation on pouring aggregate to plug horizontal tunnel with flow water. Water 12:1763. https://doi.org/10.3390/w12061763
Zheng S (2018) Application of ground directional borehole to control prevention karst collapsed column water inrush in coalmines. Coal Sci Technol 46(7):229–233
Zhu M (2015) Key technology and equipment of borehole-controlled grouting for highly effective plugging large channel of water inrush. Coalf Geol Explor 43(4):55–58
Zouaoui S, Djebouri H, Mohammedi K, Khelladi S, Aider AA (2016) Experimental study on the effects of big particles physical characteristics on the hydraulic transport inside a horizontal pipe. Chin J Chem Eng 24:317–322. https://doi.org/10.1016/j.cjche.2015.12.007

Publisher's Note